Cellular Physiology and Biochemistry

Cell Physiol Biochem 2018;51:812-826
DOI: 10.1159/000495334
Published online: 21 November 2018
Accepted: 13 November 2018

Original Paper

Catestatin Enhances Neuropathic Pain Mediated by $P2X_4$ Receptor of Dorsal Root Ganglia in a Rat Model of Chronic Constriction Injury

Zeyu Deng[a] Congcong Li[b] Errong Du[a] Chenglong Liu[a] Bihan Xia[c] Huiyu Chen[c] Qiqing He[c] Changshui Xu[a,d]

[a]Department of Physiology, Basic Medical College of Nanchang University, Nanchang, [b]The second clinical medical college of Nanchang University, Nanchang, [c]Queen Mary School, Medical Department, Nanchang University, Nanchang, [d]Jiangxi Provincial Key Laboratory of autonomic nervous function and disease, Nanchang, China

Key Words
Neuropathic pain • Catestatin • $P2X_4$ receptor • Dorsal root ganglia • Satellite glial cells • Proinflammatory cytokines • Mitogenactivated protein kinase • Nuclear factor-κB

Abstract
Background/Aims: Neuropathic pain (NPP) is the consequence of a number of central nervous system injuries or diseases. Previous studies have shown that NPP is mediated by $P2X_4$ receptors that are expressed on satellite glial cells (SGCs) of dorsal root ganglia (DRG). Catestatin (CST), a neuroendocrine multifunctional peptide, may be involved in the pathogenesis of NPP. Here, we studied the mechanism through which CST affects NPP. ***Methods:*** We made rat models of chronic constriction injury (CCI) that simulate neuropathic pain. Rat behavioral changes were estimated by measuring the degree of hyperalgesia as assessed by the mechanical withdrawal threshold (MWT) and the thermal withdrawal latency (TWL). $P2X_4$ mRNA expression was detected by quantitative real-time reverse transcription-polymerase chain reaction. $P2X_4$ protein level and related signal pathways were assessed by western blot. Additionally, double-labeled immunofluorescence was employed to visualize the correspondence between the $P2X_4$ receptor and glial fibrillary acidic protein. An enzyme-linked immunosorbent assay was performed to determine the concentration of CST and inflammatory factors. ***Results:*** CST led to lower MWT and TWL and increased $P2X_4$ mRNA and protein expression on the SGCs of model rats. Further, CST upregulated the expression of phosphor-p38 and phosphor-ERK 1/2 on the SGCs of CCI rats. However, the expression level of phosphor-JNK and phosphor-p65

Z. Deng and C. Li contributed equally to this work.

Changshui Xu
Department of Physiology, Basic Medical College of Nanchang University; Jiangxi Provincial Key Laboratory of autonomic nervous function and disease Nanchang, 330006 (China); E-Mail xuchangshui@ncu.edu.cn

did not obviously change. ***Conclusion:*** Taken together, CST might boost NPP by enhancing the sensitivity of $P2X_4$ receptors in the DRG of rats, which would provide us a novel perspective and research direction to explore new therapeutic targets for NPP.

Introduction

Considering that pain has been clinically used as the fifth vital sign after the four basic fundamental life-signs (body temperature, pulse, respiration and blood pressure) and that chronic pain itself has been identified as a kind of diseases [1, 2], the study of chronic pain is of great research significance. Nevertheless, treatments for this long-term pathological condition remain unsatisfactory. NPP that caused by nerve damage is a representative chronic pain [3].

Presynaptic dorsal root ganglia neurons relay sensory information regarding pain and express several ATP-binding purinergic receptors known collectively as $P2X_{1-7}$ [4-7]. The highly calcium-permeable $P2X_4$ receptor subtype has proven to function in the development of NPP [8], with upregulation of $P2X_4$ promoting NPP after peripheral nerve injury [9]. More specifically, activation of $P2X_4$ receptors in the DRG, causes the release of substance P and inflammatory substances, which in turn activates spinal dorsal microglia and the release of TNF-α, IL-1β, IL-6, ATP, NGF, NO, ROS, PGs, and other active neuronal substances and proinflammatory cytokines, thereby participating in the production and maintenance of NPP [10].

Catestatin (CST: human CHGA352-372, bovine CHGA344-364) is a 21-amino acid neuroendocrine peptide that is derived from the chromogranin A (CHGA) [11]. In recent years, several studies have investigated the connection between CST and inflammation/pain [12-15]. At the same time, many of the inflammatory factors involved in NPP are mediated by the $P2X_4$ receptor. This implies that CST likely affects NPP, although it has not yet been demonstrated. The aim of this study was to determine whether and how CST acts on NPP, specifically whether it acts via $P2X_4$ receptors on DRG satellite glial cells.

Materials and Methods

Animals model and groups

Healthy and clean male Sprague-Dawley rats (180–220 g) were obtained from the Laboratory Animal Science Department of Nanchang University. The rats were placed in plastic squirrel-cages after grouping and were kept under standard housing conditions (22 ± 2°C, 50% humidity, and 12-h light/dark cycle) with free access to food and water. We tried to reduce both animal suffering and the number of animals used as much as possible throughout the research. All experiments were reviewed and approved by the animal management committee of Nanchang University. Models of neuropathic pain were established by inducing chronic constriction injury in rats. Before the CCI operation, all rats (except the control rats) were intraperitoneally injected with 10% chloral hydrate (0.3 ml/100g) for anesthesia. Specific surgical procedures are described briefly as follow： First, we separated out the left mid-thigh sciatic nerves; second, four loose knots were tied in the isolated sciatic nerve with 4-0 chrome catgut. The distance between knots was about one millimeter and the tightness level of each ligation was set so that blood supply of the nerve adventitia was normal. Finally, the rats were disinfected with iodophor.

Rats were randomly divided into 7 groups: (1) control (ctrl, no operation); (2) sham operation group in which the sciatic nerve was separated without any ligation (sham); (3) CCI; (4) CCI treated with CST (CCI+CST); (5) CCI treated with scrambled CST peptide (CCI+NC); (6) CCI treated with CST-siRNA group (CCI+CST-siRNA); (7) CCI treated with the scrambled siRNA group (CCI+NC-siRNA). Each group contained six rats and all rats participated all procedures. On the 4th, 5th, and 6th days after surgery, rats in the CCI+CST group were injected intrathecally with CST (0.1 mM, Catalog No. 053-43, Phoenix, USA) dissolved in 10 μl of 0.01 M phosphate-buffered saline (PBS). The synthetic sequence of CST was Arg-Ser-Met-Lys-Leu-Ser-Phe-Arg-Ala-Arg-Ala-Tyr-Gly-Phe-Arg-Asp-Pro-Gly-Pro-Gln-Leu, and its purity was at least 95%. In the same

way, rats in the CCI+NC group were injected intrathecally with scrambled CST peptide (0.1 mM, Phoenix, USA), with a synthetic sequence of Gly-Arg-Gly-Arg-Glu-Pro-Gly-Ala-Tyr-Pro-Ala-Leu- Asp-Ser-Arg-Gln-Glu. Rats in the CCI+CST-siRNA group were injected intrathecally (0.05mg/kg) with CST-siRNA (Novobio, China) and rats in the CCI+NC-siRNA group were injected intrathecally (0.05mg/kg) with NC-siRNA (Novobio, China). The target sequences for CST-siRNA were: sense 5′-CAACAACAACACAGCACUdTdT-3′ and anti-sense 5′-AGCUGCUGUGUUGUUGUUGdTdT-3′. *In vivo* transfection reagents (Engreen, China) were used in the siRNA transduction procedure. Pain sensation (nociception) was estimated by measuring MWT and TWL. MWT and TWL were assessed on Day 0, 1, 3, 5, 7, 9, and 11 after establishing the CCI models. On the 14th day, rats from all groups were sacrificed to collect the serum and L4-6 DRGs from the operative side.

Measurement of the mechanical withdrawal threshold (MWT)

MWT assessed via stress stimulation can quantify the degree of mechanical hyperalgesia. Unrestrained rats were placed in a transparent plastic chamber (22 × 12 × 22 cm) on a stainless steel wire mesh (grid 1 × 1 cm). Before starting the trials, we kept the room at 20–25 °C and gave all rats a few minutes to explore and acclimate to the new environment. The paw withdrawal response is known to be a positive response [16, 17]. We used an Electrical Mechanical Analgesia Tester (BME-404, Tianjin, China) to stimulate their operated hind paws with pressure (range: 0–50 g). Stimulation was delivered 10 times total to each rat at 10 s intervals. We calculated the average strength of the ten measured values for each rat, and the average value for all rats in a group (n = 6) was designated as the MWT for the group. Testing was done blindly without knowing to which group rats belonged.

Measurement of the thermal withdrawal latency (TWL)

Thermal hyperalgesia was evaluated by heat stimulation. The rats were placed in a transparent, bottomless, and square acrylic box (22 × 12 × 22 cm) on a glass plate. We used a Full-automatic Plantar Analgesia Tester (BME-410C, Tianjin, China) to stimulate the operated hind paws with a heat beam that could penetrate the glass plate. The beam shut down immediately and automatically when a rat withdrew its paw. The time from beam onset to beam offset was recorded as the TWL. Withdrawal latency was measured ten times in each rat at 5 min intervals. The longest thermal stimulation lasted 30 s. As with MWT, we calculated the average length of stimulation for each rat, and the average all rats in a group (n = 6) was designated as the TWL for the group. Testing was done blindly without knowing to which group rats belonged and operated hind paws were tested.

Quantitative real-time reverse transcription-Polymerase Chain Reaction (qPCR)

L4-6 DRGs on the operated side were identified on 14th day after operation. We selected one ganglion randomly from each rat to finish the qPCR. The isolated ganglions were cleaned with 0.01 M PBS and then stored in RNA preservation solution at −80 °C before use. qPCR was performed to measure the expression level of $P2X_4$ mRNA in each group. Total RNA was extracted from isolated DRGs with a Total RNA Extraction Kit (Promega, Beijing, China). Then, 10 μl of the total RNA was incubated for 60 min at 37 °C to be reverse transcribed into complementary DNA (cDNA) using a first strand cDNA synthesis kit (Thermo Fisher Scientific lnc., USA), according to the manufacturer's instructions. After cDNA synthesis was completed, the reaction mixture was obtained using a SYBR Green PCR Kit (Qiagen, Germany). qPCR amplification was performed with StepOne Sequence Detection Software v2.3 (Applied Biosystems Inc., USA) to quantify the expression level of $P2X_4$ mRNA. The forward primer sequence was 5'-CCCTTTGCCTGCCCAGATA-3' and the reverse primer sequence was 5'-CCGTACGCCTTGGTGAGTGT-3'. Corresponding to these $P2X_4$ sequences, we chose β-actin as the internal reference, with forward and reverse primers being 5'-CCTAAGGCCAACCGTGAAAAGA-3' and 5'-GGTACGACCAGAGGCATACA-3', respectively. The key module for amplification is known to be the thermal cycle. Particularly, the reaction parameters were 95 °C for 2 min to activate DNA polymerase, 40 cycles of 2-step cycling for amplification at 95 °C for 5 s, followed by 60 °C for 30 s, and ultimately extension at 95 °C for 15 s (total volume 20 μl). We aimed to obtain the melting curve that was used to confirm the amplification specificity, and the results were analyzed by the software described above. The ΔCT value was the average $P2X_4$ value minus the average threshold cycle (CT) value for β-actin (ΔCT = CT target − CT reference). The ΔΔCT value was similarly calculated as the ΔCT value of the test sample minus the ΔCT value

of calibrator sample (ΔΔCT = ΔCT test sample − ΔCT calibrator sample). Finally, we determined the relative quantity (RQ) of $P2X_4$ expression according to the acknowledged equation: $RQ = 2^{-\Delta\Delta CT}$, and compared this value across groups.

Western blot

The L4-6 DRGs from the operated side were dissected from the different groups on the 14th day after CCI operation and stored at −80 °C before use. We selected one ganglion randomly from each rat for analysis. Western blot analysis was used to obtain $P2X_4$ receptor protein expression levels in the DRGs from each group. The tissue samples were homogenized by mechanical disruption in a mixture of RIPA lysis buffer and protease and phosphatase inhibitors and incubated on ice for 30 min. Next, the tissue homogenates were centrifuged at 12, 000×g for 15 min at 4 °C. After that, the supernatants were gathered to separate EP tubes. Before the sample buffers (250 mmol/L Tris-Cl, 200 mmol/L dithiothreitol, 10% SDS, 0.5% bromophenol blue, and 50% glycerol) were added in proportion, we detected the protein concentrations using the bicinchonininc acid protein quantitative method. The last step of protein extraction was heating the samples at 95 °C for 10 min for denaturation. Equal quantities of 30-μg protein samples were loaded on 10% polyacrylamide gel for electrophoresis separation and were transferred to 0.45 mm polyvinylidene fluoride (PVDF) membranes at 300 mA for an hour and a half after electrophoresis. The PVDF membranes were incubated in blocking buffer comprising 5% skim milk or 5% bovine serum albumin dissolved in 1×TBST buffer (10 mmol/L Tris–HCl [pH 8.0], 150 mmol/L NaCl, and 0.05% Tween-20) for 2 h at room temperature. After blocking, the primary antibodies (rabbit anti-$P2X_4$, 1:200, Alomone; mouse anti-β-actin, 1:1000, Beijing Zhongshan Biotech CO.; rabbit anti-p38, 1:1000; rabbit anti-phosphor-p38, 1:1000; rabbit anti-JNK,1:1000; rabbit anti-phosphor-JNK, 1:1000; rabbit anti-ERK1/2, 1:1000; and rabbit anti-phosphor-ERK1/2, 1:1000, rabbit anti-p65, 1:1000; rabbit anti-phosphor-p65, 1:1000, Cell Signaling Technology) were incubated with the PVDF membranes overnight at 4 °C, and then an HRP-conjugated secondary goat anti-mouse antibody or goat anti-rabbit secondary antibody (1:2000, Beijing Zhongshan Biotech CO.) were incubated with the membranes at room temperature for 1 h. An enhanced chemiluminescence kit was used to visualize the protein bands and the densities of the detected proteins were analyzed by Image-Pro Plus Software.

Double-labeled Immunofluorescence

Co-expression of the $P2X_4$ receptor with glial fibrillary acidic protein (GFAP) in the DRG was measured by double-labeled immunofluorescence. The sampling time and site were the same as what was used for the western blot experiment. We selected one ganglion randomly from each rat for immunofluorescence analysis. The DRGs were isolated from the rats and washed with 0.01 M PBS immediately. Then they were fixed in 4% paraformaldehyde (PFA) for 2 h at room temperature and washed three times with 0.01 M PBS, followed by 20% sucrose diluted in 4% PFA overnight at 4 °C. After that, successive 10-μm coronal sections were made with using a microtome at −20 °C. The tissue chips were rinsed 3 times in 0.01 M PBS for 5 min and punched with 0.3% Triton X-100 diluted in 0.01 M PBS for 15 min at room temperature to increase the permeability of antibodies to cell membrane. Then the slices were rinsed 3 times in PBS for 5 min and blocked with normal goat serum working liquid at 37 °C for 1 h to block the non-specific antigens. The sections were next incubated with the mixed primary antibodies, including antibodies against GFAP (mouse anti-GFAP, Biolegend) and $P2X_4$ 1:200 diluted in 0.01 M PBS, at 4 °C overnight. After washing 3 times in 0.01 M PBS, sections were incubated with secondary antibodies at 37 °C for 1 h. The goat anti-mouse fluorescein isothiocyanate (FITC) and goat anti-rabbit tetraethyl rhodamine isothiocyanate (TRITC) (1:200, Beijing Zhongshan Biotech CO.) were used as the mixed second antibodies. Finally, a fluorescent antifading buffer was used to examine the chips under fluorescence and confocal microscopes, and relevant images were taken to describe the co-expressions.

Enzyme linked immunosorbent assay (ELISA)

We obtained blood samples from carotid arteries when the rats were sacrificed and centrifuged them at 3, 000×g for 15 min after 30 min at room temperature. Then we collected the supernatants and discarded depositions. These serum samples were stored at −80 °C before use. Production of TNF-α, IL-1β, and CST were detected with ELISA test kits (ColorfulGene/Wksu-Bio, China). According to the manufacturer's instructions, 450 nm was regarded as the most suitable wavelength for measuring absorbance. A

multifunctional microplate reader (PerkinElmer, USA) was used to measure the OD values of each group and amounts of CST and the proinflammatory cytokines were calculated according to the respective standard curve.

Statistical analysis

SPSS 21.0 software was performed for statistical analysis of data. Significant between-group differences were evaluated by Analysis of Variance (ANOVA) with Tukey post hoc test. For the behavioral test, repeated-measures correction was carried out by a repeated-measurement ANOVA. Experimental data are expressed as mean ± standard error (SE). $P<0.05$ was considered to be statistically significant.

Results

CST increased the mechanical and thermal pain sensitivity in CCI rats

NPP is a chronic state of developed mechanical and thermal hyperalgesia. Before the operation, all rats had normal MWT (Fig. 1A) and TWL (Fig. 1B). We conducted a normal distribution test and a homogeneity test for all data on the Day 0. ANOVA indicated no significant differences in MWT or TWL between across groups: all $P> 0.05$. The effect of CST on MWT and TWL in CCI rats was tested at different time points after the surgical procedure (Day 0, 1, 3, 5, 7, 9, and 11 after surgery). MWT for the control and sham groups did not differ across days (all $P>0.05$). MWT for the CCI group was significantly lower than the control group postoperatively (all $P<0.01$). MWT did not significantly differ among the CCI, CCI+NC, CCI+NC-siRNA, CCI+CST, and CCI+CST-siRNA groups on Day 1, 3, or 5 (all $P>0.05$). However, MWT was much lower in the CCI+CST group than in the CCI group from Day 7 through Day 11 (all $P<0.01$). In contrast, MWT was significantly greater in the CCI+CST-siRNA group than in the CCI+CST from Day 7 through Day 11 (all $P<0.01$). MWT did not significantly differ among the CCI, CCI+NC, and CCI+NC-siRNA groups at any time points (all $P>0.05$). The corresponding measurements for TWL showed the same trend. Thus, we conclude that CST increased the mechanical and thermal pain sensitivity in CCI rats.

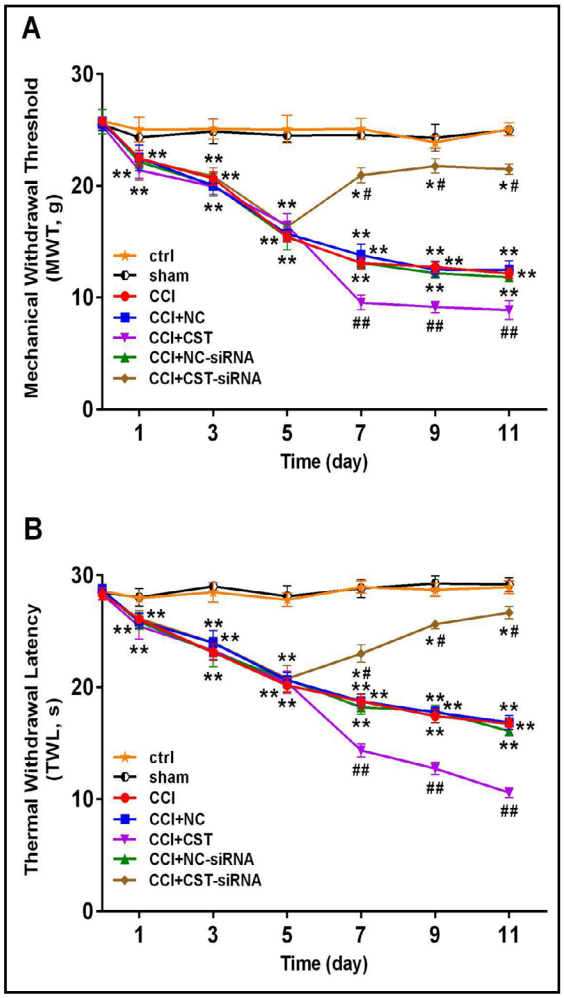

Fig. 1. CST raised the mechanical and thermal pain sensitivity of CCI rats. A, CST raised the mechanical pain sensitivity of CCI rats. B, CST enhanced the thermal pain sensitivity of CCI rats. Data were presented as mean ± SE of six animals per group. **P<0.01, vs. ctrl group, ##P<0.01, vs. CCI group,*#P<0.01, vs. CCI+CST group.

CST increased the expression of $P2X_4$ mRNA in the DRGs of CCI rats

Real-time PCR analysis was used to determine $P2X_4$ mRNA levels in the DRG (Fig. 2). The expression of $P2X_4$ mRNA was significantly lower in the control group than in the CCI group ($P<0.01$), but did not differ from expression levels in the

sham group (P>0.05). $P2X_4$ mRNA expression was significantly higher in the CCI+CST group than in the CCI group (P<0.01), but did not significantly differ among the CCI, CCI+NC, and CCI+NC-siRNA groups (all P>0.05). However, expression was much lower in the CCI+CST-siRNA group than in the CCI+CST group (P<0.01). These results indicate that CST induced expression of $P2X_4$ mRNA in the DRGs of CCI rats.

CST increased the expression of $P2X_4$ protein in the DRGs of CCI rats

Western blot analysis was used to determine the expression of $P2X_4$ protein in the DRG (Fig. 3). $P2X_4$ protein levels were significantly lower in the control group than in the CCI group (P<0.01), but did not differ from those in the sham group (P>0.05). No differences in $P2X_4$ protein levels were found among the CCI, CCI+NC, and CCI+NC-siRNA groups (all P>0.05). Protein levels were significantly higher in the CCI+CST group than in the CCI group (P<0.01) and were significantly lower in the CCI+CST-siRNA group than in the CCI+CST group (P<0.01). These results show that CST enhanced the expression of $P2X_4$ protein in the DRGs of CCI rats.

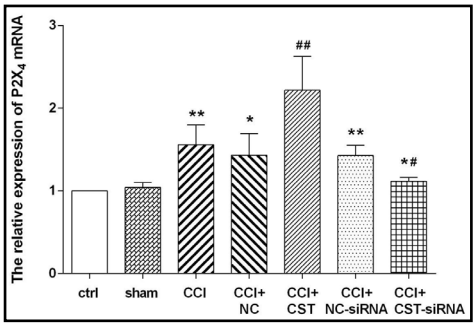

Fig. 2. CST increased $P2X_4$ mRNA level in the DRGs of CCI rats. Data were presented as mean ± SE, n=6; *P<0.05, vs. ctrl group, **P<0.01, vs. ctrl group, $^{\#\#}$P< 0.01, vs. CCI group, $^{*\#}$P<0.01, vs. CCI+CST group.

Effects of CST on activation of MAPKs in the DRGs of CCI rats

We also used western blot analyses to detect the expression of phosphor-p38, p38, phosphor-JNK, JNK, phosphor-ERK1/2, and ERK1/2 in the DRG. Quantification via western blot allowed statistical analysis of phosphorylation levels of MAPK-p38, MAPK-JNK, and MAPK-ERK1/2. As shown in Fig. 4, the integral optical density ratios of p38 (40 kd), JNK (54/46 kd), and ERK1/2 (44/42 kd) to β-actin (41.6 kd) did not differ significantly across groups (all P>0.05). Phosphorylation levels of p38 MAPK signaling was lower in the control group than in the CCI, CCI+NC, or CCI+NC-siRNA groups (all P<0.01; Fig. 4A), but did not differ from those in the sham group (P>0.05). Additionally, phosphorylation was significantly higher in the CCI+CST group than in the CCI group (P<0.01), but did not differ among the CCI, CCI+NC, and CCI+NC-siRNA groups (all P>0.05). Furthermore, phosphorylation levels of the p38 MAPK signaling were lower in the CCI+CST-siRNA group than in the CCI+CST group (P<0.01). ERK1/2 phosphorylation levels followed the same tendency (Fig. 4B). However, the expression of phosphor-JNK presented a different trend (Fig. 4C). JNK phosphorylation levels were lower in the control group than in the CCI group (P<0.01), but did not differ

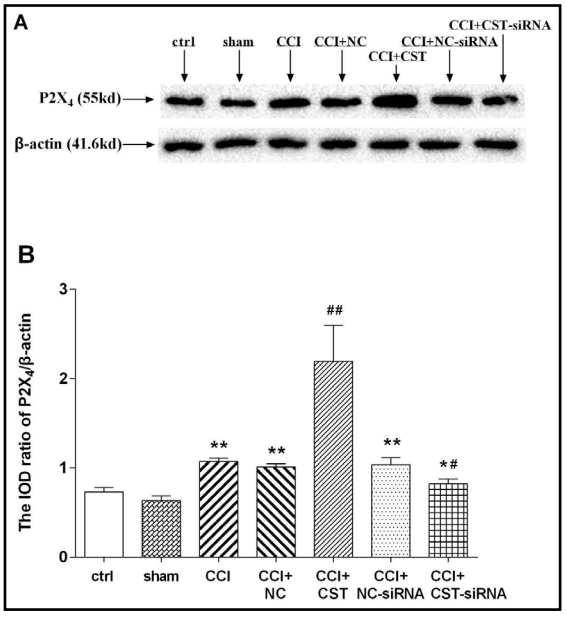

Fig. 3. CST enhanced the $P2X_4$ protein expression in the DRGs of CCI rats. A, Representative protein bands showed SDS-PAGE electrophoresis of western blot for $P2X_4$ receptor (55kd) and β–actin (41.6kd) in the same sample. B, Protein expression statistical graphs of each band whose density was normalized to its corresponding β–actin. Data were presented as mean ± SE, n=6; **P<0.01, vs. ctrl group, $^{\#\#}$P<0.01, vs. CCI group, $^{*\#}$P<0.01, vs. CCI+CST group.

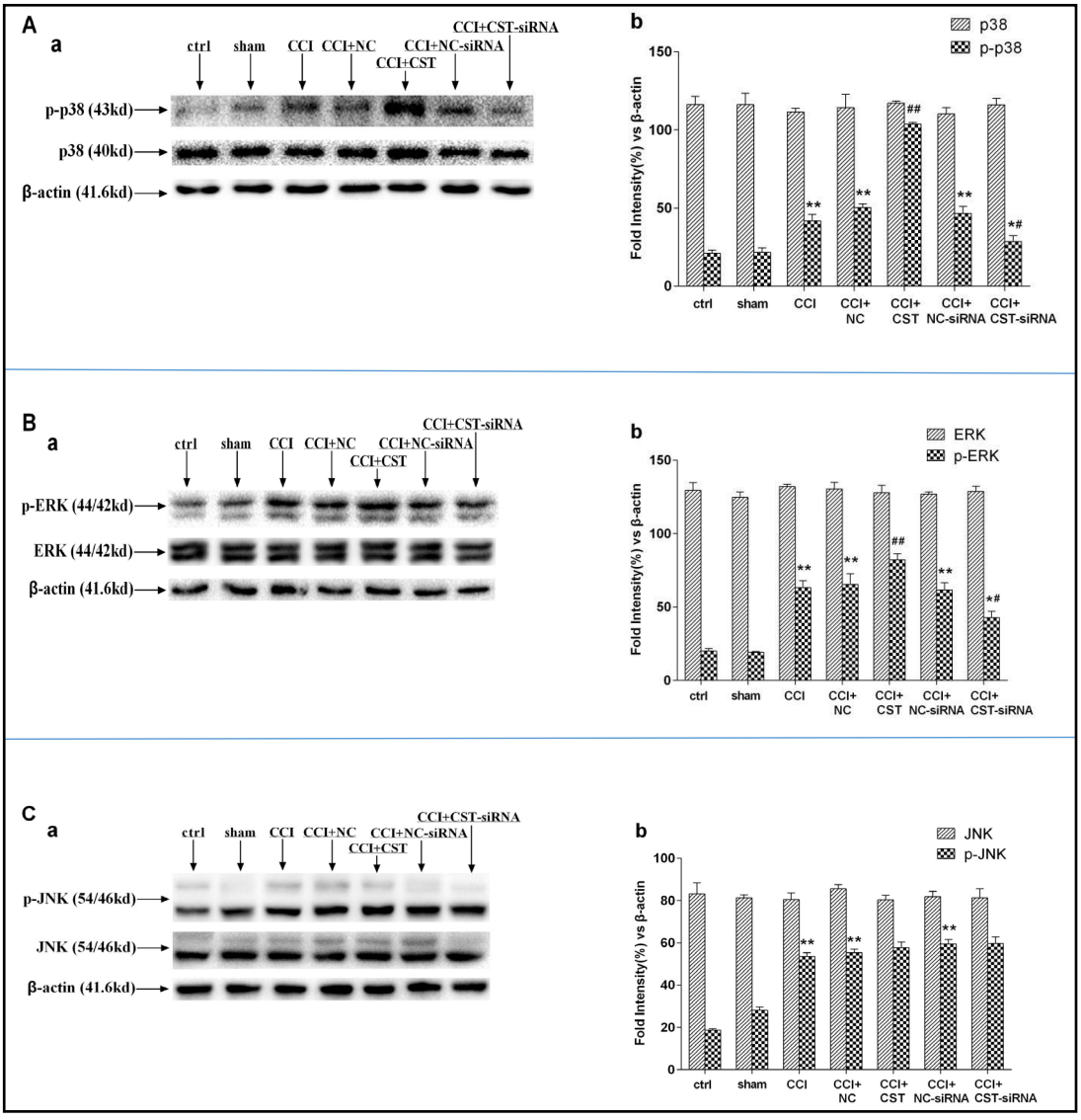

Fig. 4. The expression of phosphor-p38, phosphor-ERK and phosphor-JNK proteins in the DRGs of CCI rats. A, CST boosted the phosphorylation level of p38 signaling of CCI rats. a, Protein bands of related factors showed phosphorylation level of the p38 MAPK signal pathway detected by western blot. b, Quantification of western blot significantly demonstrated phosphorylation level of the p38 MAPK signal pathway. B, CST augmented the phosphorylation level of ERK1/2 signaling of CCI rats. a, Representative protein bands exhibited the expression on the phosphorylation level of ERK1/2 signal pathway assessed by western blot. b, Quantized histogram illuminated the integral optical density ratio of ERK1/2 and phosphor-ERK1/2 to the corresponding β-actin in the same sample. C, CST was irrelevant to the phosphorylation level of JNK pathway in CCI rats. a, Shown were representative blots of phosphor-JNK and total-JNK assessed by western blot. b, Densitometric quantitation of phosphorylation level for JNK pathway following normalization to its corresponding β-actin in the same sample. Data were presented as mean ± SE, n=6; **P<0.01, vs. ctrl group, ##P<0.01, vs. CCI group, *#P<0.01, vs. CCI+CST group.

from those in the sham group (P>0.05). JNK phosphorylation levels did not differ among the CCI, CCI+NC, and CCI+NC-siRNA groups (all P>0.05). Moreover, JNK phosphorylation did not statistically differ between the CCI+CST and the CCI groups (P>0.05) or between the CCI+CST-siRNA and CCI+CST groups (P>0.05). In summary, CST induced phosphorylation levels of p38 and ERK1/2, but had no effect on the phosphorylation expression of JNK. This suggests that

CST-induced phosphorylation of p38 and ERK1/2 might be involved in CST-induced $P2X_4$ receptor expression, and thus participate in NPP.

Effects of CST on activation of NF-κB in the DRGs of CCI rats

We analyzed the expressions of phosphorylated p65 and total p65 using western blot (Fig. 5). Statistical analysis indicated no significant differences among in p65 across groups (all $P>0.05$). Phosphor-p65 expression in the control group was lower than in the CCI group ($P<0.01$), but not different from the sham group ($P>0.05$) or among the CCI, CCI+NC, CCI+CST, CCI+NC-siRNA, and CCI+CST-siRNA groups (all $P> 0.05$). Thus, CST did not affect the phosphorylation expression of NF-kB subunit p65, which indicated that CST's effect on $P2X_4$ expression was not associated with the NF-kB p65 signaling pathway.

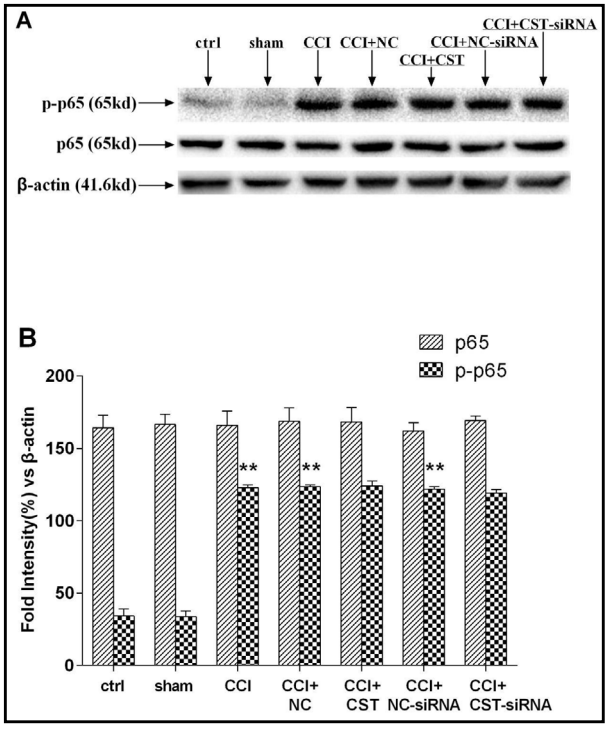

Fig. 5. The expression of phosphor-p65 and p65 proteins in the DRGs of CCI rats. A, Representative protein bands showed the phosphorylation level of NF-KB subunit p65 signal pathway detected by western blot. B, phosphor-p65 and p65 expression was normalized to its corresponding β–actin of each band exhibited in statistical graphs. Data were presented as mean ± SE, n=6; **P<0.01, vs. ctrl group.

Fig. 6. Co-expression of $P2X_4$ and GFAP in the DRGs of CCI rats. The picture illustrated the co-expressions of $P2X_4$ receptor and GFAP in six groups by double-labeled immunofluorescence. A, The co-expression of $P2X_4$ receptor and GFAP under the fluorescent microscopy for 4-fold observation. Scale bar: 50 μm. B, Amplification of positive area in Fig. 6A under the confocal microscopy (20-fold observation). Scale bar: 10μm. The green signal represents GFAP stained with FITC, and the red signal indicates $P2X_4$ stained with TRITC. The yellow color visualized in the merged image represents the $P2X_4$ and GFAP double staining image. The arrows indicate the positive cells in the DRGs.

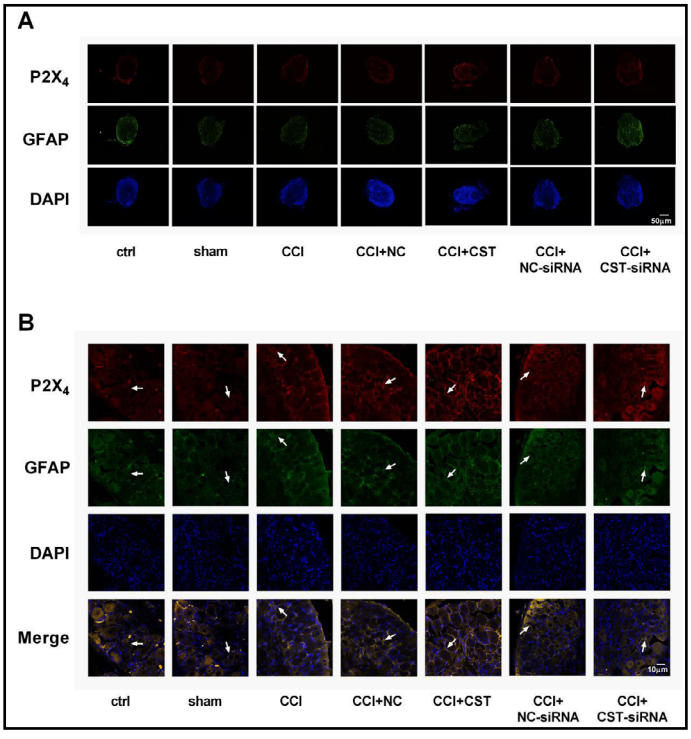

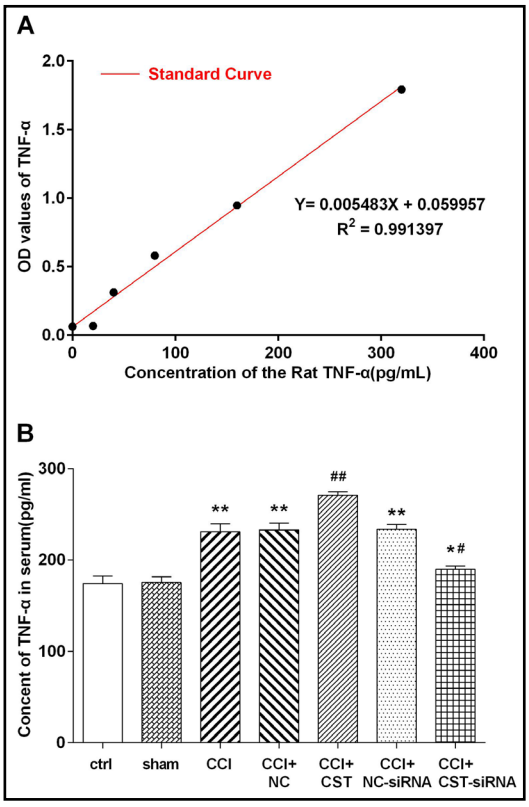

Fig. 7. CST increased TNF-α levels in the serum of CCI rats. A, Linear regression equation shows the relationship between the O.D. values at the wavelength of 450 nm and the concentrations of rat serum TNF-α. B, Quantification of ELISA demonstrated the relative content level of TNF-α in each group. Data were presented as mean ± SE. n=6, **P<0.01, vs. ctrl group, ##P<0.01, vs. CCI group, *#P<0.01, vs. CCI+CST group.

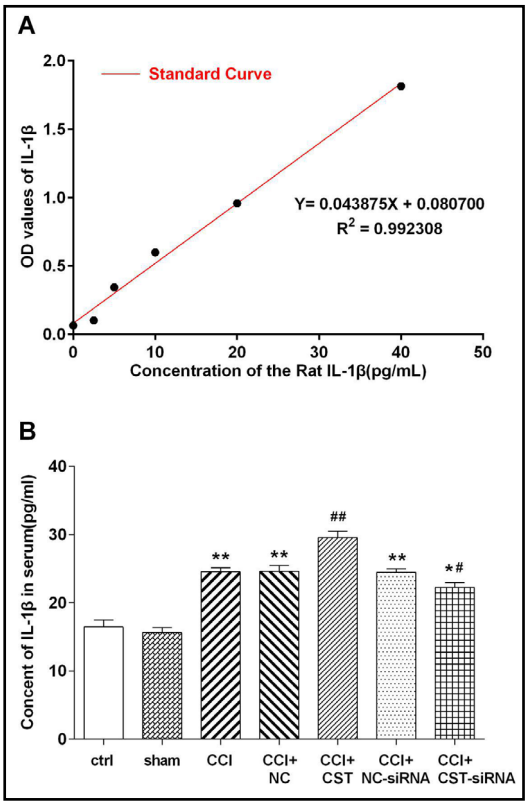

Fig. 8. CST increased IL-1β levels in the serum of CCI rats. A, Linear regression equation shows the relationship between the O.D. values at the wavelength of 450 nm and the concentrations of rat serum IL-1β. B, Quantification of ELISA demonstrated the relative content level of IL-1β in each group. Data were presented as mean ± SE. n=6, **P<0.01, vs. ctrl group, ##P<0.01, vs. CCI group, *#P<0.01, vs. CCI+CST group.

CST increased the co-expression of $P2X_4$ receptor and GFAP in the DRGs of CCI rats

Glial fiber acidic protein (GFAP) is a marker for SGCs and its upregulation indicates SGC activation. The co-expression of $P2X_4$ receptor and GFAP in the CCI rats was shown by double-labeled immunofluorescence analysis (Fig. 6). We examined DRG cross-sectional images at low magnification (Fig. 6A), and zoom in on a positive area in Fig. 6B. The green signal represents GFAP stained with FITC and the red signal indicates $P2X_4$ stained with TRITC. The yellow color visualized in the merged image represents the co-expression of $P2X_4$ and GFAP. Co-expression in the CCI group was greater than in the control group, but did not differ between the control and sham groups. Co-expression was higher the CCI+CST group than in the CCI group, but did not differ among the CCI, CCI+NC, and CCI+NC-siRNA groups. In contrast, it was significantly lower in the CCI+CST-siRNA group than in the CCI+CST group. Thus, CST distinctly promoted the production of $P2X_4$ receptor in side activated SGCs.

CST increased the TNF-α and IL-1β levels in the serum of CCI rats

We also observed greater production of TNF-α (Fig. 7) and IL-1β (Fig. 8) in serum samples of CCI rats. The concentration of serum TNF-α (pg/ml) in the CCI group was greater than that in the control group (P<0.01), while control and sham groups did not differ (P>0.05). In addition, serum TNF-α levels were higher in the CCI+CST group than in the CCI group (P<0.01), but did not differ among the CCI, CCI+NC, and CCI+NC-siRNA groups (all P>0.05).

Again, TNF-α levels in the CCI+CST-siRNA group were lower than those in the CCI+CST group (P<0.01). The same trend and statistical differences applied to IL-1β. These results suggested that CST could induce the $P2X_4$ receptor to mediate a strong inflammatory response.

CST-siRNA inhibited CST production in the serum of CCI rats

We detected the concentration of CST (ng/ml) in all groups by ELISA. The results are shown in Fig. 9. The concentration of CST in the CCI group was greater than that in the control group (P<0.01), while the control and sham groups did not differ (P> 0.05). Additionally, CST levels were prominently higher in the CCI+CST group than in the CCI group (P<0.01), while they did not differ among the CCI, CCI+NC, and CCI+NC-siRNA groups (all P>0.05). However, CST levels in the CCI+CST-siRNA group were markedly lower than those in the CCI group (P<0.01). Thus, analysis showed that CST-siRNA could interfere and reduce CST production in CCI rats.

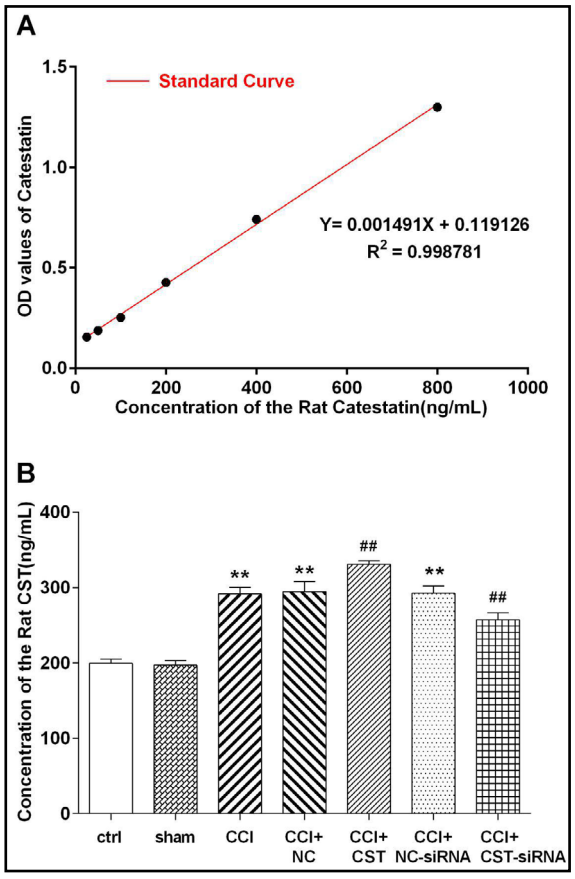

Fig. 9. CST-siRNA inhibited CST expression in the serum of CCI rats. A, Linear regression equation shows the relationship between the O.D. values at the wavelength of 450 nm and the concentrations of rat CST. B, Quantification of ELISA demonstrated the relative content level of CST in each group. Data were presented as mean ± SE of six animals per group. n=6, **P<0.01, vs. ctrl group, ##P<0.01, vs. CCI group.

Discussion

As a pain syndrome caused by injury or disease of the nervous system, NPP often brings about at least one of the following pathological manifestations: spontaneous pain, secondary pain, allodynia, hyperalgesia, or ongoing pain [18, 19]. NPP is usually accompanied by the damage, dysfunction, or injury of the peripheral and central nervous systems [20, 21]. Ectopic discharge occurs when DRG neurons are damaged, which is a key factor in the development of NPP [22]. DRG neurons receive most of the primary sensory input from the body as the primary sensory ganglia. The massive impact of injured DRG neurons can alter spinal synaptic plasticity or lead to central sensitization (hyperalgesia or allodynia) [23]. Sensory ganglia of rats contain the stomata of sensory neurons and SGCs that closely surround these neurons, with SGCs being an important part of the painsignal-transduction pathway [22, 24, 25]. Traditional NPP treatment is barely satisfactory, and some evidence suggests that glial cells might be a more appropriate therapeutic target [26-29]. The $P2X_4$ receptor is similar to a cation-selective ion-channel receptor and has high permeability to Ca^{2+}; it is mainly distributed in the spinal cord microglia and DRG satellite glial cells [30, 31]. When the expression of the $P2X_4$ receptor on the surface of activated glia is upregulated, the result is abnormal pain, indicating that the $P2X_4$ receptor is closely related to NPP [32, 33]. We used a CCI model that could finely simulate the clinical state of NPP [34]. CST has been show to inhibit nicotine-evoked catecholamine secretion [35, 36]. Apart from functioning as a nicotinic cholinergic antagonist to restrain catecholamine release, CST also takes active part

in a wide range of pathophysiology processes, such as innate immunity, inflammatory and autoimmune reactions, several homeostatic regulations, and cardiovascular modulations [37-40]. Here, the behavioral test results showed that the CCI group exhibited significantly lower MWT and TWL than in the control group from the 1st to the 11th day after operation, indicating that the models of neuropathic pain were successfully established. Interestingly, after CST injection, the MWT and TWL of the CCI+ CST group became even lower than those of the CCI group. Therefore, CST might enhance pain sensitivity in CCI rats, and deeper experiments were performed to explain this phenomenon. Any form of damage (e.g., transection of axons or inflammation) can cause abnormal SGCs activation marked increased GFAP expression [41-43]. GFAP is generally regarded as a sign of SGC activation and is almost absent in resting states [44, 45]. Immunofluorescence results showed that co-expression of the $P2X_4$ receptor and GFAP in SGCs was higher in the CCI+CST group than in the CCI group, indicating that CST might affect $P2X_4$ receptor expression that is related to SGC activation in the DRG. qPCR and western blot results showed that the expression levels of $P2X_4$ mRNA and protein in the DRG were significantly greater in the CCI+CST group than in the CCI group, which further illustrates this point. The main finding of our study was that expression of the $P2X_4$ receptor on SGCs in the DRG increased significantly after intrathecal injection of CST in CCI rats. This indicates that CST might enhance $P2X_4$ receptor expression, thus exciting DRG neurons and resulting in greater pain sensitivity in CCI rats. Additionally, in peripheral nerve inflammation/injury, activated glial cells would release proinflammatory factors, which excite neurons and cause NPP [46, 47]. According to ELISA quantitative detection, serum TNF-α and IL-1β were both significantly higher in the CCI rats than in control rats, and much higher in the CCI+CST group than in the CCI group, which implies that CST stimulated the increase in these cytokines. We also showed that CST-siRNA blocked CST production in the serum of CCI rats, which also supports these results. Taken together, these findings suggest that CST enhances the sensitivity of $P2X_4$ receptors in the satellite glial cells of the DRG, which acts to exacerbate NPP. CST acts as an inflammation mediator by activating a variety of signal transduction pathways, including PI3 kinase, NO and MAPK dependent pathways [48]. p38, c-Jun N-terminal kinase (JNK), and extracellular signal-regulated kinase (ERK1/2) form the MAPK family in mammals. The MAPK family is widely expressed serine/tyrosine kinases that play an important role in many signaling pathways in mammalian cells [49]. Under some instances of pain, MAPKs in glial cells help increase synthesis and release of proinflammatory cytokines [50, 51]. Each MAPK signaling pathway has a different role depending on the circumstances [52-54]. Considering the MAPKs are a fundamental part of inflammation [55], here, we tested whether they were activated with western blot. The result showed that CST activated the p38 and ERK MAPK pathways to increase $P2X_4$ receptor expression. As for JNK, the JNK signal pathway was reported to be activated more rapidly than other MAPKs involved in NPP [56]. The expression of phosphor-JNK in the CCI model group was higher than in the control group, which agrees with a previous study [57]. However, expression levels of phosphor-JNK did not differ between the CCI+CST and CCI groups. This indicates that CST mediated the development of NPP by activating the p38 and ERK signaling pathways, but not the JNK signaling pathway. NF-kB is another classic signaling pathway associated with inflammation. The activation of NF-kB was reported to be higher in the DRGs of sciatic nerve-injured rats and was vital to hyperalgesia associated with the NF-kB subunits p50/p65 [58, 59]. Because the p65 subunit of NF-kB was reported to be associated with NPP [60]; we examined total p65 and phosphorylated p65 using western blot. Phosphor-p65 expression was higher in the CCI group than in the control group, but did not differ from levels in the CCI+CST group. We concluded that NF-kB did not participate in process through which CST regulates NPP.

Conclusion

In summary, CST treatment can aggravate NPP by giving rise to abnormal excitatory transmission in DRG neurons. The effect is mediated by the $P2X_4$ receptor on the surface of SGCs. The concrete mechanism is likely to be that CST activates the $P2X_4$ receptor via the p38 and ERK pathways. Activation of the $P2X_4$ receptor then increases the release of TNF-α and IL-1β, which participate in the maintenance and development of NPP.

Acknowledgements

We are particularly grateful to those who have contributions to our study. We would like to thank the Laboratory Animal Science Department of Nanchang University for providing experimental animals. This work was supported by the grant (Nos.: 81660199, 81260187) from the National Natural Science Foundation of China, and the grant (No.: 20153BCB23033) from the Cultivating Foundation of Young Scientists (Star of Jinggang) of Jiangxi Province. We also thanked Shangdong Liang, Ph.D., in Nanchang University who participated in this study.

Disclosure Statement

The authors declare no conflicts of interest with respect to the research, authorship, and/or publication of this article.

References

1 Mukherjee P, Cinelli MA, Kang S, Silverman RB: Development of nitric oxide synthase inhibitors for neurodegeneration and neuropathic pain. Chem Soc Rev 2014;43:6814-6838.
2 Uchida H, Ma L, Ueda H: Epigenetic gene silencing underlies C-fiber dysfunctions in neuropathic pain. J Neurosci 2010;30:4806-4814.
3 Smith BH, Torrance N, Bennett MI, Lee AJ: Health and quality of life associated with chronic pain of predominantly neuropathic origin in the community. Clinical Journal of Pain 2007;23:143.
4 Chaban VV: Visceral sensory neurons that innervate both uterus and colon express nociceptive TRPv1 and P2X3 receptors in rats. Ethn Dis 2008;18:S2-20-24.
5 Cook SP, McCleskey EW: Cell damage excites nociceptors through release of cytosolic ATP. Pain 2002;95:41-47.
6 Hamilton SG, McMahon SB: ATP as a peripheral mediator of pain. J Auton Nerv Syst 2000;81:187-194.
7 Burnstock G: P2X receptors in sensory neurones. British Journal of Anaesthesia 2000;84:476-488.
8 Bernier LP, Ase AR, Seguela P: P2X receptor channels in chronic pain pathways. British Journal of Pharmacology 2018;175:2219-2230.
9 Ulmann L, Hatcher JP, Hughes JP, Chaumont S, Green PJ, Conquet F, Buell GN, Reeve AJ, Chessell IP, Rassendren F: Up-regulation of P2X4 receptors in spinal microglia after peripheral nerve injury mediates BDNF release and neuropathic pain. J Neurosci 2008;28:11263-11268.
10 Verma V, Singh N, Singh Jaggi A: Pregabalin in neuropathic pain: evidences and possible mechanisms. Curr Neuropharmacol 2014;12:44-56.
11 Bandyopadhyay GK, Vu CU, Gentile S, Lee H, Biswas N, Chi NW, O'Connor DT, Mahata SK: Catestatin (chromogranin A(352-372)) and novel effects on mobilization of fat from adipose tissue through regulation of adrenergic and leptin signaling. J Biol Chem 2012;287:23141-23151.
12 Deng Z, Xu C: Role of the neuroendocrine antimicrobial peptide catestatin in innate immunity and pain. Acta Biochim Biophys Sin (Shanghai) 2017;49:967-972.
13 Rabbi MF, Labis B, Metz-Boutigue MH, Bernstein CN, Ghia JE: Catestatin decreases macrophage function in two mouse models of experimental colitis. Biochem Pharmacol 2014;89:386-398.

14 Rabbi MF, Eissa N, Munyaka PM, Kermarrec L, Elgazzar O, Khafipour E, Bernstein CN, Ghia JE: Reactivation of Intestinal Inflammation Is Suppressed by Catestatin in a Murine Model of Colitis via M1 Macrophages and Not the Gut Microbiota. Frontiers in Immunology 2017;8:985.
15 Ying W, Mahata S, Bandyopadhyay GK, Zhou Z, Wollam J, Vu J, Mayoral R, Chi NW, Webster NJG, Corti A, Mahata SK: Catestatin Inhibits Obesity-Induced Macrophage Infiltration and Inflammation in the Liver and Suppresses Hepatic Glucose Production Leading to Improved Insulin Sensitivity. Diabetes 2018;67:841-848.
16 Van BM, Hermes D, Honig WM, Linderoth B, Smj VK, Van KM, Joosten EA: Long-Term Spinal Cord Stimulation Alleviates Mechanical Hypersensitivity and Increases Peripheral Cutaneous Blood Perfusion in Experimental Painful Diabetic Polyneuropathy. Neuromodulation Journal of the International Neuromodulation Society 2018;doi: 10.1111/ner.12757.
17 Diniz L, Portella VG, Da KSA, Araújo P, De RAJ, Cavalcante ADA, Coelhodesouza AN, Lealcardoso JH: Electrophysiologic alterations in the excitability of the sciatic and vagus nerves during early stages of sepsis. Journal of Pain Research 2018;11:783-791.
18 Navarro A, Saldana MT, Perez C, Torrades S, Rejas J: A cost-consequences analysis of the effect of pregabalin in the treatment of painful radiculopathy under medical practice conditions in primary care settings. Pain Practice : the Official Journal of World Institute of Pain 2011;11:31-41.
19 Stanos SP, Galluzzi KE: Topical therapies in the management of chronic pain. Postgrad Med 2013;125:25-33.
20 Ochoa JL: Neuropathic pain: redefinition and a grading system for clinical and research purposes. Neurology 2009;72:1282-1283.
21 Jensen TS, Baron R, Haanpaa M, Kalso E, Loeser JD, Rice AS, Treede RD: A new definition of neuropathic pain. Pain 2011;152:2204-2205.
22 Devor M: Ectopic discharge in Abeta afferents as a source of neuropathic pain. Exp Brain Res 2009;196:115-128.
23 Lee MC, Nam TS, Jung SJ, Gwak YS, Leem JW: Modulation of Spinal GABAergic Inhibition and Mechanical Hypersensitivity following Chronic Compression of Dorsal Root Ganglion in the Rat. Neural Plast 2015;2015:924728.
24 Huang TY, Hanani M: Morphological and electrophysiological changes in mouse dorsal root ganglia after partial colonic obstruction. Am J Physiol Gastrointest Liver Physiol 2005;289:G670-678.
25 Jasmin L, Vit JP, Bhargava A, Ohara PT: Can satellite glial cells be therapeutic targets for pain control? Neuron Glia Biol 2010;6:63-71.
26 Costa FA, Moreira Neto FL: Satellite glial cells in sensory ganglia: its role in pain. Rev Bras Anestesiol 2015;65:73-81.
27 Ji RR, Berta T, Nedergaard M: Glia and pain: is chronic pain a gliopathy? Pain 2013;154 Suppl 1:S10-28.
28 Milligan ED, Watkins LR: Pathological and protective roles of glia in chronic pain. Nat Rev Neurosci 2009;10:23-36.
29 Tsuda M, Kuboyama K, Inoue T, Nagata K, Tozaki-Saitoh H, Inoue K: Behavioral phenotypes of mice lacking purinergic P2X4 receptors in acute and chronic pain assays. Mol Pain 2009;5:28.
30 Kobayashi K, Yamanaka H, Noguchi K: Expression of ATP receptors in the rat dorsal root ganglion and spinal cord. Anat Sci Int 2013;88:10-16.
31 Kobayashi K, Fukuoka T, Yamanaka H, Dai Y, Obata K, Tokunaga A, Noguchi K: Differential expression patterns of mRNAs for P2X receptor subunits in neurochemically characterized dorsal root ganglion neurons in the rat. J Comp Neurol 2005;481:377-390.
32 Smith HS: Activated microglia in nociception. Pain Physician 2010;13:295-304.
33 Tsuda M, Tozaki-Saitoh H, Inoue K: Purinergic system, microglia and neuropathic pain. Curr Opin Pharmacol 2012;12:74-79.
34 Ding W, You Z, Shen S, Yang J, Lim G, Doheny JT, Chen L, Zhu S, Mao J: An Improved Rodent Model of Trigeminal Neuropathic Pain by Unilateral Chronic Constriction Injury of Distal Infraorbital Nerve. J Pain 2017;18:899-907.
35 Mahata SK, O'Connor DT, Mahata M, Yoo SH, Taupenot L, Wu H, Gill BM, Parmer RJ: Novel autocrine feedback control of catecholamine release: A discrete chromogranin a fragment is a noncompetitive nicotinic cholinergic antagonist. J Clin Invest 1997;100:1623-1633.

36 Mahapatra NR, O'Connor DT, Vaingankar SM, Hikim AP, Mahata M, Ray S, Staite E, Wu H, Gu Y, Dalton N, Kennedy BP, Ziegler MG, Ross J, Mahata SK: Hypertension from targeted ablation of chromogranin A can be rescued by the human ortholog. J Clin Invest 2005;115:1942-1952.
37 Sahu BS, Obbineni JM, Sahu G, Allu PK, Subramanian L, Sonawane PJ, Singh PK, Sasi BK, Senapati S, Maji SK, Bera AK, Gomathi BS, Mullasari AS, Mahapatra NR: Functional genetic variants of the catecholamine-release-inhibitory peptide catestatin in an Indian population: allele-specific effects on metabolic traits. J Biol Chem 2012;287:43840-43852.
38 Kojima M, Ozawa N, Mori Y, Takahashi Y, Watanabe-Kominato K, Shirai R, Watanabe R, Sato K, Matsuyama TA, Ishibashi-Ueda H, Koba S, Kobayashi Y, Hirano T, Watanabe T: Catestatin Prevents Macrophage-Driven Atherosclerosis but Not Arterial Injury-Induced Neointimal Hyperplasia. Thromb Haemost 2018;118:182-194.
39 Angelone T, Quintieri AM, Brar BK, Limchaiyawat PT, Tota B, Mahata SK, Cerra MC: The Antihypertensive Chromogranin A Peptide Catestatin Acts as a Novel Endocrine/Paracrine Modulator of Cardiac Inotropism and Lusitropism. Endocrinology 2008;149:4780-4793.
40 Theurl M, Schgoer W, Albrecht K, Jeschke J, Egger M, Beer AG, Vasiljevic D, Rong S, Wolf AM, Bahlmann FH: The neuropeptide catestatin acts as a novel angiogenic cytokine via a basic fibroblast growth factor-dependent mechanism. Circulation Research 2010;107:1326-1335.
41 Woodham P, Anderson PN, Nadim W, Turmaine M: Satellite cells surrounding axotomised rat dorsal root ganglion cells increase expression of a GFAP-like protein. Neurosci Lett 1989;98:8-12.
42 Berta T, Liu T, Liu YC, Xu ZZ, Ji RR: Acute morphine activates satellite glial cells and up-regulates IL-1beta in dorsal root ganglia in mice via matrix metalloprotease-9. Mol Pain 2012;8:18.
43 Warwick RA, Hanani M: The contribution of satellite glial cells to chemotherapy-induced neuropathic pain. Eur J Pain 2013;17:571-580.
44 Blum E, Procacci P, Conte V, Sartori P, Hanani M: Long term effects of lipopolysaccharide on satellite glial cells in mouse dorsal root ganglia. Exp Cell Res 2017;350:236-241.
45 Hanani M: Satellite glial cells in sensory ganglia: from form to function. Brain Res Brain Res Rev 2005;48:457-476.
46 Inoue K: [Neuropharmacological study of ATP receptors and their role in neuropathic pain]. Yakugaku Zasshi 2013;133:1035-1039.
47 Cohen SP, Mao J: Neuropathic pain: mechanisms and their clinical implications. BMJ 2014;348:f7656.
48 Egger M, Beer AG, Theurl M, Schgoer W, Hotter B, Tatarczyk T, Vasiljevic D, Frauscher S, Marksteiner J, Patsch JR, Schratzberger P, Djanani AM, Mahata SK, Kirchmair R: Monocyte migration: a novel effect and signaling pathways of catestatin. Eur J Pharmacol 2008;598:104-111.
49 Marie Cargnello PPR: Activation and Function of the MAPKs and Their Substrates, the MAPK-Activated Protein Kinases. Microbiology & Molecular Biology Reviews Mmbr 2011;75:50-83.
50 Moy JK, Khoutorsky A: The MNK-eIF4E Signaling Axis Contributes to Injury-Induced Nociceptive Plasticity and the Development of Chronic Pain. The Journal of Neuroscience : the Official Journal of the Society for Neuroscience 2017;37:7481-7499.
51 Wang Z, Ma W, Chabot JG, Quirion R: Cell-type specific activation of p38 and ERK mediates calcitonin gene-related peptide involvement in tolerance to morphine-induced analgesia. Faseb j 2009;23:2576-2586.
52 Kim EK, Choi EJ: Compromised MAPK signaling in human diseases: an update. Arch Toxicol 2015;89:867-882.
53 Obata K, Yamanaka H, Dai Y, Tachibana T, Fukuoka T, Tokunaga A, Yoshikawa H, Noguchi K: Differential activation of extracellular signal-regulated protein kinase in primary afferent neurons regulates brain-derived neurotrophic factor expression after peripheral inflammation and nerve injury. J Neurosci 2003;23:4117-4126.
54 Manassero G, Repetto IE, Cobianchi S, Valsecchi V, Bonny C, Rossi F, Vercelli A: Role of JNK isoforms in the development of neuropathic pain following sciatic nerve transection in the mouse. Mol Pain 2012;8:39.
55 Peluso I, Yarla NS, Ambra R, Pastore G, Perry G: MAPK signalling pathway in cancers: Olive products as cancer preventive and therapeutic agents. Semin Cancer Biol 2017;doi: 10.1016/j.semcancer.2017.09.002.
56 Obata K, Yamanaka H, Kobayashi K, Dai Y, Mizushima T, Katsura H, Fukuoka T, Tokunaga A, Noguchi K: Role of mitogen-activated protein kinase activation in injured and intact primary afferent neurons for mechanical and heat hypersensitivity after spinal nerve ligation. The Journal of Neuroscience : the Official Journal of the Society for Neuroscience 2004;24:10211-10222.

57 Zhuang ZY, Wen YR, Zhang DR, Borsello T, Bonny C, Strichartz GR, Decosterd I, Ji RR: A peptide c-Jun N-terminal kinase (JNK) inhibitor blocks mechanical allodynia after spinal nerve ligation: respective roles of JNK activation in primary sensory neurons and spinal astrocytes for neuropathic pain development and maintenance. Journal of Neuroscience 2006;26:3551-3560.

58 Chan CF, Sun WZ, Lin JK, Lin-Shiau SY: Activation of transcription factors of nuclear factor kappa B, activator protein-1 and octamer factors in hyperalgesia. European Journal of Pharmacology 2000;402:61-68.

59 Ma W, Bisby MA: Increased activation of nuclear factor kappa B in rat lumbar dorsal root ganglion neurons following partial sciatic nerve injuries. Brain Research 1998;797:243-254.

60 Marchand F, Perretti M, Mcmahon SB: Role of the immune system in chronic pain. Nature Reviews Neuroscience 2005;6:521-532.